Available online at www.sciencedirect.com

ScienceDirect

journal homepage: www.elsevier.com/locate/cose

Computers & Security

Source camera identification for re-compressed images: A model perspective based on tri-transfer learning

Guowen Zhang[a], *Bo Wang*[a,*], *Fei Wei*[b], *Kaize Shi*[a], *Yue Wang*[a], *Xue Sui*[c], *Meineng Zhu*[d]

[a] *School of Information and Communication Engineering, Dalian University of Technology, P.R. China*
[b] *Department of Electrical Engineering, The State University of New York at Buffalo, Buffalo, NY 14260-2500 USA.*
[c] *Liaoning Normal University, Dalian, Liaoning, 116029, P.R. China*
[d] *Beijing Institute of Electronics Technology and Application, Beijing, 100091, P.R. China*

ARTICLE INFO

Article history:
Received 27 April 2020
Revised 12 August 2020
Accepted 5 October 2020
Available online 8 October 2020

Keywords:
Source camera identification (SCI)
Tri-transfer learning
Prototype construction
Double JPEG compression
Co-training

ABSTRACT

Source Camera Identification (SCI) achieves high accuracy on matching identification, in which the training and testing sample sets are derived from the same statistical distribution. However, in practice the training and testing sets, namely, the source and test domains, may consist of digital images that are double compressed by various software and applications with different quantization tables. Unfortunately, existing methods are inadequate in performance under such circumstances, such that we aim to find an algorithm that can fill the gap between the training and testing sets. In this work, we propose an algorithm, tri-transfer Learning (TTL), which is a cross-pollination of transfer learning and tri-training. For TTL, the transfer learning module transfers the knowledge learned from the training sets to improve the identification performance on testing. Compared with other methods, TTL uses a semi-supervised approach requiring only a small number of training samples and has better performance than other methods. The tri-training module, which is a variation of the co-training, facilitates knowledge transferring by assigning pseudo-labels to unlabelled instances and adds target instances with labels to the training set in batches. Combining the two modules, our framework can gain higher efficiency and performance than other state-of-art methods on mismatched camera model identification which is supported by experiments based on the open-source Dresden Image Database.

1. Introduction

With the development of modern technologies, the popularity of smart devices with high-resolution cameras is growing. With the growth of online social media and networks, digital images play an important role in daily life. Additionally, digital images are taken as evidence by the justice system. However, with numerous applications in the market, digital image editing is no longer a professional skill, such that it is easy to tamper or forge digital images without visible traces. Recently, there have been several events with considerable negative effects that involve tampered and forged digital images that have harmed the public credence in the media and press. Under this circumstance, a challenge arises, that is, can we identify the authenticity and source of a forensic image? The frequent use of digital media as critical evidence has led to the rapid development of multimedia forensics in the last decade Stamm et al. (2013). SCI, which is an important

* Corresponding author.
E-mail address: bowang@dlut.edu.cn (B. Wang).
https://doi.org/10.1016/j.cose.2020.102076

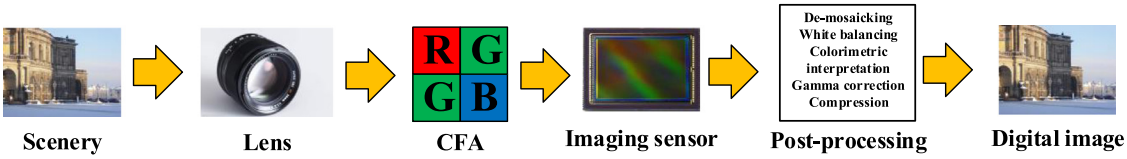

Fig. 1 – Imaging pipeline in a digital camera.

branch of multimedia forensics, aims to identify and authenticate the source device of a given image Kharrazi et al. (2004). Many methods have been proposed and we can categorize most works on SCI into two categories: camera individual identification and camera model identification Piva (2013).

1.1. *Camera individual identification*

The basic methods of camera individual identification mostly focus on sensor pattern noise. Due to the manufacturing imperfection, the difference in the size of the photodiode and the parameters of the MOS FET in each pixel structure may cause minor distortion in the pixel output signal. Researchers consider those indelible marks left by the camera as defects that can be used as fingerprints to identify the source camera. Thus, individual camera identification often uses SPN methods. Lukas *et al.* Lukas et al. (2005) demonstrated the feasibility of using sensor pattern noise from images for digital camera identification. The pattern noise is extracted from images using a wavelet-based denoising filter and they average the noise obtained from several images to determine the camera patterns, which serve as the fingerprints. Evidently, the more accurate the SPN is, the higher the identification accuracy. Therefore, researchers attempt to extract more accurate SPNs by assigning weighting factors according to the magnitude of scene details or adopting adaptative filters Hu et al. (2009); Kang et al. (2012); Lawgaly et al. (2013); Li (2010); Lukas et al. (2006); Sutcu et al. (2007); Wu et al. (2012).

The multimedia forensic community has studied SPN-based source camera identification for more than a decade. Many existing SPN-based methods have achieved a high detection accuracy on SCI. However, limitations affect the performance of the SPN-based methods Li (2016). Specifically, the characteristics produced in the imaging acquisition process can impact the purity of the SPN and the content of the image can also contaminate the SPN. In addition, to obtain the prior information of source cameras, images taken by the test cameras are required. As a matter of fact, this is not a fully blind forensics method.

1.2. *Camera model identification*

Most existing methods for camera model identification are based on statistical features and follow a framework that regards camera model identification as a classification problem. Statistical traces, such as white balancing, JPEG compression and colour filter array in the images have the potential to link the images to the source camera models. Fig. 1 illustrates the process of acquiring an image with a digital camera. These statistical features are often used to construct the training set for classifiers such as support vector machines (SVMs) or ensemble classifiers. The features are specific for the camera model, such that they are often used for camera model identification. A detailed discussion of the methods of camera model identification is given in Section 2.

Although most statistical-feature-based camera model identification methods can achieve high detection accuracy, there are still some limitations. One limitation is that most of the methods are trained and tested in an ideal environment in which the training and testing sets are derived from the same distribution. However, in practice, digital images are more likely to be double compressed when they are uploaded to the Internet through apps, e.g., Facebook, Twitter and Instagram. In scenarios in which the training set and testing set mismatches, namely, the training and testing samples are recompressed separately with different quantizations, the performance of the existing methods declines dramatically due to the difference in statistical feature distributions between the training and testing sets. One solution is obtaining sufficient labels for the testing samples, but that is time and labour consuming which is not acceptable commercially.

1.3. *Our work*

In this paper, to address camera model identification in a more practical scenario in which the training samples and testing samples are double compressed by different quantization tables, we propose an algorithm, tri-transfer Learning which combines transfer learning and tri-training, a variant of co-training to eliminate the difference between the source and target distributions. Our method seeks to adapt the training set from the target domain to the source domain to transfer the knowledge from target domain to the training set. In addition, our algorithm reduces the required accuracy for the pseudo-labels at the initial iteration of the co-training and does not need any labelled sample in the target domain compared with other algorithms that combine transfer learning and co-training.

- *Transfer learning* is used to bridge the gap between the source domain and the target domain to make the distributions of the statistical features in the two domains closer.
- *Tri-training* helps to assign the unlabelled instances in the target domain to the source domain (training set) with the pseudo-labels.

In the field of camera model identification, this is the first work using unlabelled samples with pseudo-labels to facilitate knowledge in the source domain. The rest of the paper is organized as follows. In Section 2, we introduce some related work. In Section 3, our proposed method will be presented in

detail with pseudocode. In Section 4, we present our experiments and compare our results with competitors. Finally, we conclude in Section 5.

2. Previous works

2.1. Statistical feature-based camera model identification

In the work proposed by Kharrazi Kharrazi et al. (2009), the features used for camera model identification consist of image quality metrics (IQM), average pixel value, wavelet domain statistics, neighbour distribution centre of mass, RGB pair energy ratio and pair correlation. An experiment on 5 different camera models achieveed an average accuracy of 88.02%. As JPEG compression is widely used by consumer-level cameras, Kai *et al.*, Kai et al. (2007) examined the JPEG compression statistics left in the images for identifying the source camera model. They used the number of bits per pixel and the percentage of non-zero integers in each discrete cosine transform (DCT) coefficient to capture the correlation between the quality and size of a certain camera model. Kai *et al.* Kai et al. (2006) use the lens radial distortion and combine the statistics obtained from image intensities to classify the camera models. Gloe *et al.* Gloe et al. (2009) tested the performance of feature-based camera model identification on a large set of cameras from an in-depth analysis on the intra-camera model similarity, the number of required devices and images for training, and the effect of camera setting. Their experiments showed that feature-based camera model identification works in practice and provides reliable results. Wang *et al.* Wang et al. (2009) used the higher-order wavelet features and wavelet coefficient co-occurrence features from taken images and applied the sequential forward feature selection method to reduce the redundancy and correlation of features. Wang et al. (2009) achieved a prominent improvement in identification ability, especially for different models of the camera same brand with an average accuracy of 96% on 6 camera models.

Xu *et al.* Xu and Shi (2012) used the uniform grayscale invariant local binary pattern (LBP) from spatial domain of red and green channels, the corresponding prediction-error arrays and the 1st-level diagonal wavelet sub-bands of each image. The proposed scheme can capture the characteristics of image processing algorithms such as JPEG compression, demosaicking and filtering. The average accuracy of the LBP is 98.08%. Ojansivu *et al.* Ojansivu and Heikkil (2008) proposed a local phase quantization (LPQ) texture analysis in which the phases of the four low-frequency coefficients are uniformly quantized into one of 256 hypercubes in an 8-dimensional space by operating on the Fourier phase computed locally for a window on every image position. Then a histogram collecting LPQ codes for all image pixel neighbourhoods is obtained. Inspired by Ojansivu and Heikkil (2008); Xu and Shi (2012), Xu *et al.* Xu et al. (2016) proposed to extracting local binary patterns (LBP) from the original image, the residual noise image, and the contourlet transform coefficients of the residual noise images. They also extracted LPQ features from the original image and the residual noise image. It was shown that the method using combined texture features extracted from HSV colour space has a better detection accuracy.

The colour filter array (CFA) modes and demosaicing algorithms are different in cameras from different brands and can be used for identification. Bayram *et al.* Bayram et al. (2005) proposed identifying the source camera based on traces of the colour interpolation algorithm. In their work, the estimation of the interpolation coefficients, which designates the amount of contribution from each pixel in the interpolation kernel, was obtained by the expectation maximization algorithm. Then the interpolation coefficients, the peak location, and the magnitudes are combined as the feature. However, the CFA pattern of an image is unknown and we must try various CFA models and interpolation algorithms. John *et al.* Ho et al. (2010) developed a method to measure the correlations between the colour channels and construct a v-map to match an image to its source. It achieved promising results and addresses the problem of the unknown CFA pattern.

Some features of very high dimensions are also used for identification. Roy *et al.* Roy et al. (2017) proposed a discrete cosine transform residual (DCTR) that effectively captures the JPEG compression artefacts imposed in the images by the quantization table used for JPEG compression. Then the combination of the random forest-based ensemble classification and the PCA-based dimensionality is used to improve the classification accuracy for which the average accuracy obtained is 97.08%. Chen *et al.* Chen and Stamm (2015) united a set of submodels to build a rich model of the camera demosaicing algorithm. For each CFA pattern and interpolating algorithm, they utilized two co-occurrence matrices to capture the reconstruction error between the original image and the reconstructed version. With all the co-occurrences merged, a 1372-dimensional feature was obtained.

Although those works have good performances, they still suffer from double JPEG compression. Our work aims to address the problem by reducing the difference between the distributions of training and testing datasets.

2.2. Co-training

Co-training was first proposed by Blum and Mitchell Blum and Mitchell (1998) who trains two classifiers on independent views (features) and used the most confident unlabelled samples of each other to augment the training data. The idea of co-training, which utilizes natural redundancy, has been widely employed in many other fields. The standard co-training algorithm requires two sufficient and redundant views. Dasgupta *et al.* Dasgupta et al. (2002) showed that when the requirement is met, the algorithm could makes fewer generalizations. Inspired by Blum and Mitchell (1998), Nigam *et al.* Nigam and Ghani (2000) showed that co-training algorithms are both discriminative in nature and robust to the assumptions of their embedded classifiers. Simultaneously, they proposed a new algorithm combining the co-training and expectation maximization (co-EM) that improves the performance. To address the high requirement of co-training, Zhou and Li Zhou and Li (2005) proposed a new co-training style semi-supervised method named tri-training. The method employs three clas-

Table 1 – Different transfer learning settings.

Transfer Learning Settings	Related Areas	Source Domain Labels	Target Domain Labels	Tasks
Inductive Transfer Learning	Multi-task Learning	Available	Available	Regression Classification
	Self-taught Learning	Unavailable	Available	Regression Classification
Transductive Transfer Learning	Domain Adaptation, Sample Selection Bias, Co-variate Shift	Available	Unavailable	Regression Classification
Unsupervised Transfer Learning	*	Unavailable	Unavailable	Clustering, Dimensionality Reduction

sifiers and can gracefully choose examples to label by using multiple classifiers to compose the final hypothesis.

Co-training is also widely used in many practical data mining applications. Kiritchenko *et al.* Nigam and Ghani (2000) addressed the lack of labelled data in email classification by exploring co-training with a support vector machine (SVM). In biometrics, Bhatt *et al.* Bhatt et al. (2011) used co-training to update classifiers with labelled as well as unlabelled instances. Hwa *et al.* Hwa et al. (2003) proposed an approach called one-sided corrected co-training that requires manually annotated decisions to address the problem, for which the parse is usually a complicated structure and not easy to label.

2.3. *Transfer learning*

The mismatched problem of target and source data distribution also exists in other research areas, such as text classification and computer vision. The training and testing data are defined as the source and target domains, respectively. Pan and Yang Pan and Yang (2010) surveyed the history of transfer learning, and presented a unified definition of transfer learning that categorizes transfer learning into three different settings (given in Table 1).

Some methods focus on using multi-task Learning to fill the gap between the source domain and target domain. Chen *et al.* Chen et al. (2011) proposed an algorithm named co-training for domain adaptation (CODA) to slowly add both the target features and instances to the training set in which the current algorithm is most confident. CODA outperforms on the 12-domain benchmark dataset of Blitzer *et al.* Blitzer et al. (2007). In cross-lingual sentiment classification, Wan Wan (2009) proposed a co-training approach to make use of unlabelled Chinese data to solve the limitation of the number of Chinese sentiment corpora by exploring the correlation between English corpora and Chinese corpora. Ng *et al.* Ng et al. (2012) proposed a co-transfer learning algorithm using a graph-based method to use the labelled data from different feature spaces to enhance the classification of different learning spaces simultaneously. The approach is supervised and transfers the knowledge based on the affinities computed with co-occurrence information. Zhao *et al.* Zhao and Hoi (2010) proposed the online transfer learning (OTL) to transfer knowledge from the source domain to an online learning task on a target domain with an ensemble in a supervised manner using incrementally labelled instances from the target domain. Inspired by Zhao and Hoi (2010), Bhatt *et al.* Bhatt et al. (2014) proposed co-transfer learning (CTL) which is a cross-pollination of transfer learning and co-training by changing the weights of the ensemble classifiers. However, the ensemble classifiers, in their framework, cannot be applied to our challenge of source camera model identification with fewer labelled samples in the target domain used at the beginning.

Researchers have also focused on projecting the original features of the two domains to another subspace by exploring the correlations between the training and testing dataset. Pan *et al.* Pan et al. (2011) proposed the transfer component analysis (TCA) to learn a transformation that can minimize the difference of the distributions in the projected feature subspaces. Long *et al.* Long et al. (2014) proposed an algorithm named joint distribution adaptation (JDA) to simultaneously reduce both the marginal and conditional distribution differences of two domains in the projected subspace.

For the mismatched camera model identification problem, Zhang *et al.* Zhang et al. (2017) proposed a transformation based on the Gaussian model to minimize the difference between the source and target domains. However, the effectiveness of the method is quite limited. We found that the accuracies of the algorithms decrease rapidly with the increasing difference of quantization tables in the source and target domains. We will compare this method with tri-transfer learning in our work.

3. The proposed method

Humans can transfer knowledge among related tasks, which makes humans capable of quickly learning a new task related to previous learning experiences. However, in the context of camera model identification, traditional algorithms do not have such ability in that they are unable to use prior knowledge from a related task, which may help to learn new tasks efficiently. Tri-transfer learning attempts to help algorithms to gain such ability. As we addressed previously, in practice, labelled data in a double-compressed target domain is scarce, such that obtaining labels from a such target domain is expensive and time consuming, and learning an effective model is difficult. However, a large number of unlabelled samples are available to help learn the model.

In our method, transfer learning and tri-training are applied jointly to transfer the knowledge from the source domain to the target domain. Selecting the ”positive” samples at a very low classification accuracy is the problem that we hope to solve. As shown in Fig. 2, tri-training updates the training

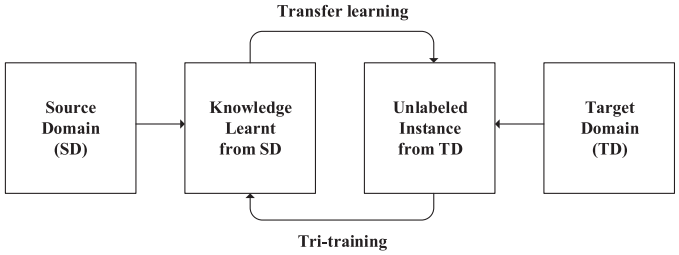

Fig. 2 – Illustration of the tri-training process from the source domain to the target domain.

data in classifiers with unlabelled samples in the target domain.

We assume that the data originate from two domains, the source (training set) and target (testing set) domains. The images in the two domains are different in quantization tables. The data in the source domain are denoted by $D_s^l = \{(x_1^S, y_1^S) \ldots, (x_n^S, y_n^S)\}$ and samples from distribution $P_S(X, Y)$. For each instance, x_i has three views $\{x_{i,1}, x_{i,2}, and x_{i,3}\}$ and a label $y_i \in \{1, 2 \ldots, m\}$. $x_{i,1}$, $x_{i,2}$, $and x_{i,3}$ represent the input vectors from three separate views (features) that are utilized for tri-training and m represents the number of camera model categories. The target data are sampled from $P_T(X, Y)$, and all samples are unlabeled and denoted as $D_T^u = \{(x_1^T) \ldots, (x_{n_t}^T)\}$.

Our goal is to train the classifiers $\hbar(x)$ to accurately predict the labels on the unlabelled samples of D_T^u, and extend them to out-of-sample test samples.

3.1. *Sufficient and redundant*

Good diversity can significantly improve the performance of ensemble learning and with co-training is concerned, there are many methods for increasing diversity between learners that can be easily generalized to tri-training.

- Blum and Mitchell Blum and Mitchell (1998) first proposed co-training based on naive bayes (NB), which requires two sufficient and redundant features subsets. Therefore, page-based and hyperlink-based feature subsets are established in the two co-training learners, respectively. The final output is determined by the posterior probability of combined learners.
- In some fields, it is difficult to obtain two sufficient and redundant feature subsets, which means there are no natural attributes. As a result, single-view co-training was proposed in Zhou and Goldman (2004). This kind of co-training splits a whole feature set into two sufficient and redundant feature subsets and establishes learners on each feature.
- Inspired by bagging, Zhou *et al*. Zhou and Li (2005) achieved diversity by manipulating the original labelled example set. Specifically, the initial training dataset is trained from datasets generated via bootstrapping sampled from the original labelled sample set.
- Additionally, Goldman and Zhou Goldman and Zhou (2000) achieved diversity by using different supervised learning algorithms and the method does not require sufficient and redundant views.

For the application of diversity in camera model identification, there are many sufficient and redundant views. In additon, bagging is applied to increase the diversity in our algorithm.

3.2. *Tri-transfer learning*

Inspired by transfer learning and co-training, we design a method to identify the double-compressed images with mismatched training samples. The co-training algorithm is shown in Algorithm 1.

Algorithm 1 Description of co-training.

Require:
A learning problem with two views $\mathbf{V_1}$ and $\mathbf{V_2}$;
A learning algorithm $\hbar$;
The sets T and U of labelled and unlabelled examples;
The number k of the iterations to be performed;
Co − training:
1: For k iterations;
2: Use $\hbar$, $V_1(T)$ and $V_2(T)$ to create classifiers h_1 and h_2
3: For each class C_i:
Let E_1 and E_2 be α unlabelled examples on which h_1 and h_2 make the most confident predictions for C_i.
Remove E_1 and E_2 from U. label them according to h_1 and h_2, respectively, and add them to T.
4: Combine the prediction of h_1 and h_2.

To combine the co-training and transfer learning in mismatched source camera model identification, we should address two challenges. First, unlike other algorithms combining the co-training and transfer learning, our method does not use any information in the target domain. Second, the more challenging work is that the initial accuracy of classifiers is often very low, which means that the pseudo-labels for the most confident samples of classifiers are probably wrong. Sometimes, all the images in the target domain may be classified into the same category. Our work aims to address the challenges of proposing an effective method by improving co-training to tri-training which differs from the method in Zhou and Li (2005). As shown in the Fig. 3, the source domain classifiers h_A, h_B, $and h_C$ are trained with sufficient labelled training data denoted by $D_s^l = \{(x_1^S, y_1^S) \ldots, (x_n^S, y_n^S)\}$. Every classifier corresponds to a view (feature). U_A, U_B, $and U_C$ are unlabelled samples from the target domain and are in the different feature spaces. In the iteration, I_a, I_b, $and I_c$ are the unlabeled data selected from U_A, U_B, $and U_C$, respectively.

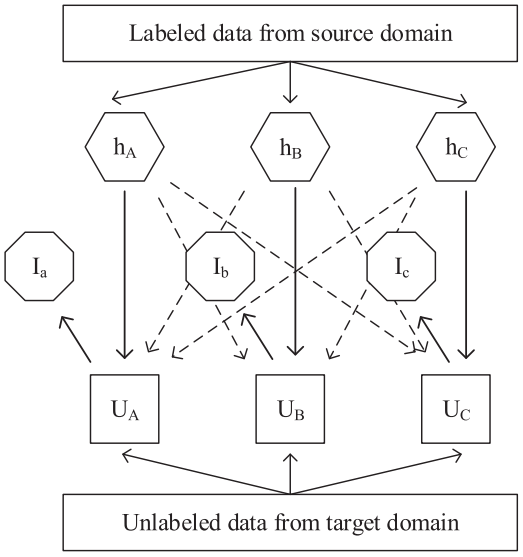

Fig. 3 – Block diagram illustrating the steps of tri-transfer learning.

For instance, using the classifier h_A, we can obtain a set of samples in U_A with $P(\hat{y}_i|x)_A$ sorting from high to low. I_a is the most confident sample set chosen from U_A with constraint $h_B(x) = \hat{y}_i$ or $h_C(x) = \hat{y}_i$. Here, confidence means that $P(\hat{y}_i|x)_A$ is relatively high in the samples. The constrain helps to ensure that pseudo-labels are correct. Then, I_a is transformed into the training data of h_B and h_C. The proposed tri-transfer learning algorithm for the camera model identification is shown in Algorithm 2.

In the original co-training formulation Blum and Mitchell (1998), it is assumed that the two views of the data are conditionally independent of classes. This assumption is strong and not applicable in practice. Balcan *et al.* Balcan et al. (2005) relaxed the requirement significantly to a condition of ϵ-expandability. For the two classifiers which that can teach each other, they must make confident predictions on different subsets of the unlabelled U. Following Chen et al. (2011), we define $C_i(x)_A$ as a confidence indicator function (for same confidence threshold $\tau > 0$). For $i \in \{1, 2, 3, 4\}$, we define

$$C_i(x)_A = \begin{cases} 1, & if\ P(\hat{y}_i|x)_A > \tau \\ 0, & otherwise \end{cases} \tag{1}$$

Similarly, we define $C_i(x)_B$, $C_i(x)_C$ for $i \in \{1, 2, 3, 4\}$. The ϵ-expanding condition can be explained as follows. For any two out of the three classifiers that meet the requirement, for example, h_A and h_B:

$$\sum_{x\in U}\sum_{i}\left[(C_i(x)_A\bar{C}_i(x)_B + \bar{C}_i(x)_A C_i(x)_B)\right] \geq \epsilon min\left[\sum_{x\in U}\sum_{i} C_i(x)_A C_i(x)_B, \sum_{x\in U}\sum_{i}\bar{C}_i(x)_A\bar{C}_i(x)_B\right] \tag{2}$$

Here, $\bar{C}_i(x)_A = 1 - C_i(x)_A$ indicates that the classifier h_A is not confident about the input x. Intuitively, the constraint in equation(7) ensures that the input U can be used for iteration because exactly one classifier is confident, which indicates some degree of independence between the two views in the set U.

Algorithm 2 Tri-transfer learning.

Input: U_s^l labelled samples from source domain
U_t^u labelled samples from target domain
h_A classifier-based view 1.
h_B classifier-based view 2.
h_C classifier-based view 3.
for $i \in \{1\ldots, 3\}$(number of views) **do**
$U_i \leftarrow BooststrapSample(U_t^u)$
$L_i \leftarrow BooststrapSample(U_s^l)$
endfor
repeat until does not satisfy the formula
1: Allocate $U_1 = U_A, U_2 = U_B, U_3 = U_C$ and $L_1 = L_A, L_2 = L_B, L_3 = L_C$ and $I_1 = I_a, I_2 = I_b$ and $I_3 = I_c$
2: Use h_A to train on L_A, use h_B to train on L_B and use h_C to train on L_C
3: Use h_A, h_B and h_C separately to predict each data x in U_A, U_B and U_C : $h_A(x), h_B(x)$ and $h_C(x)$. In addition we can obtain the class probability estimation $P(\hat{y}_i|x)_A, P(\hat{y}_i|x)_B$ and $P(\hat{y}_i|x)_C$
4: Update I_a, I_a is chosen from U_A which has relatively high $P(\hat{y}_i|x)_A$ with the constraint $h_B(x) = \hat{y}_i$ or $h_C(x) = \hat{y}_i$
5: Update I_b, I_b is chosen from U_B which has relatively high $P(\hat{y}_i|x)_B$ with the constraint $h_A(x) = \hat{y}_i$ or $h_C(x) = \hat{y}_i$
6: Update I_c, I_c is chosen from U_C which has relatively high $P(\hat{y}_i|x)_C$ with the constraint $h_A(x) = \hat{y}_i$ or $h_B(x) = \hat{y}_i$
7: Update $L_A = L_A + I_b + I_c, L_B = L_B + I_a + I_c$ and $L_C = L_C + I_a + I_b$
8: Remove I_a, I_b, and I_c from U_A, U_B and U_C
end of repaet
Output: $h(x) \leftarrow \arg\max_{y\in label} \sum_{i:h_i(x)=y} 1$

3.3. *Analysis*

For co-training, some work Angluin and Laird (1988); Goldman and Zhou (2000); Zhou and Li (2005) has theoretically analysed the feasibility. Here, we simply analyse the feasibility of the tri-transfer learning algorithm theoretically. In tri-training, three classifiers h_A, h_B and h_C choose unlabelled data to recover the labels and the recovered data are considered as the new labeled data. We assume that $|L|$ labelled data are in the classifier after $(t-1)$ iterations and $|L_t|$ are the new recovered data in the t-th iteration. Therefore, after t iterations, the training data size becomes $|L \bigcup L_t|$. Let η_L be the noise rate in the original label data L. $e_1^{\sim t}$ denotes the upper bound of the classification error rate in $|L_t|$. Hence we obtain the classification noise in the t-th iteration:

$$\eta_t = \frac{\eta_L|L| + e_1^{\sim t}|L_t|}{|L \bigcup L_t|} \tag{3}$$

The works in Angluin and Laird (1988); Xu et al. (2012) proposed that when the recovered data (with predicted labels) in the $(t+1)$-th iteration have relatively smaller noise compared with labelled data $e_1^{\sim t+1} < \eta_t$, the learning hypothesis can achieve lower error rate, which implies $\varepsilon_{t+1} < \varepsilon$. Here, the error rate of the learning hypothesis ε is denoted as:

$$\varepsilon \propto \eta \tag{4}$$

At the beginning of the iteration, the constraint of tri-transfer learning makes $e_1^{\sim 1} < \eta_L$. After every iteration, with the correctly recovered samples ($x \epsilon U_t^u$), the distribution of training data ($P_M(X, Y)$) in the classifiers is closer to the target domain compared with the distribution of source data which is:

$$|P_M(X,Y) - P_T(X,Y)| < |P_S(X,Y) - P_T(X,Y)| \tag{5}$$

We conclude that $e_1^{\sim t+1} < e_1^{\sim t}$. Intuitively, the noise from the $(t+1)$-th iteration is smaller than the classification noise rate in the t-th iteration.

$$e_1^{\sim t+1} < \frac{\eta_t |L| + e_1^{\sim t} |L_t|}{|L \bigcup L_t|} \tag{6}$$

Note that the newly labelled data in each iteration are different, so $|L \bigcup L_t \bigcup L_{t+1}| = |L \bigcup L_t| \bigcup |L_{t+1}|$, then we deduce:

$$\frac{\eta_L |L| + e_1^{\sim t} |L_t| + e_1^{\sim t+1} |L_{t+1}|}{|L \bigcup L_t| \bigcup |L_{t+1}|} < \frac{\eta_t |L| + e_1^{\sim t} |L_t|}{|L \bigcup L_t|} \tag{7}$$

Based on eq(7), we obtain $\eta_{t+1} < \eta_t$. Finally, $\varepsilon_{t+1} < \varepsilon_t$ is proven.

4. Experiments

In this section, we conduct extensive experiments to evaluate tri-transfer learning method on mismatched source camera model identification. We perform our algorithm based on CFA Bayram et al. (2005), LBP Xu and Shi (2012) and EDF Chen and Stamm (2015). Then, we compare our method with several current forensic methods, co-training and the transformation in Zhang et al. (2017). We ensemble classifiers Kodovsky et al. (2012) as basic classifiers and our method can be generalized to other fields with any learning algorithm. Even in the case that has only two views (A and B), we can change the constraint to $h_B(x) = \hat{y}_i$ for viewing A and $h_A(x) = \hat{y}_i$ for viewing B.

4.1. *Experimental setup*

4.1.1. *Datasets*

We evaluate our algorithm on a public image database, the "Dresden Image Database" Gloe and Bhme (2010). The database introduces and documents a novel image database specifically built for the development and benchmarking of camera-based digital forensic techniques Gloe and Bhme (2010). We remove the camera categories without sufficient images and choose 17 camera models from popular camera bands from the database. The details can be found in Table 2.

4.1.2. *Details*

In our experiments, because image sizes vary in the database, we extract LBP from the 512 × 512 subimage cropped from the upper left corner, EDF from the 512 × 512 subimage cropped from the upper left corner and CFA from the 256 × 256 subimage cropped from the centre. For every learner, we use 100 samples from the source domain as the initial training samples. The comparison algorithms are co-training Blum and Mitchell (1998) and CCAZhang et al. (2017). For co-training, we choose two features, EDF and LBP as the views that have higher initial accuracy. Table 2 shows the setting of classifiers for every view. The comparison algorithms have the same setting as TTL. For the CCA, we follow the initialization of the data in the paper in equation(8).

Table 2 – Camera models used in the experiment.

Camera Model	Resolution	Format	Train/Test
Agfa_DC-30i	3264 × 2448	JPEG	100/200
Agfa_Sensor505_x	2592 × 1944	JPEG	100/200
Canon_Ixus70	3072 × 2304	JPEG	100/200
Casio_EX-Z150	3264 × 2448	JPEG	100/200
FujiFilm_FinePixJ50	3264 × 2448	JPEG	100/200
Kodak_M1063	3664 × 2748	JPEG	100/200
Nikon_D70s	3008 × 2000	JPEG	100/200
Nikon_CoolPixS710	4352 × 3264	JPEG	100/200
Olympus_mju_1050SW	3648 × 2736	JPEG	100/200
Panasonic_DMC_FZ50	3648 × 2736	JPEG	100/200
Pentax_OptioA40	4000 × 3000	JPEG	100/200
Praktica_DCZ5.9	2560 × 1920	JPEG	100/200
Ricoh_GX100	3648 × 2736	JPEG	100/200
Rollei_RCP_7325XS	3072 × 2304	JPEG	100/200
Samsung_L74wide	3072 × 2304	JPEG	100/200
Samsung_NV15	3648 × 2736	JPEG	100/200
Sony_DSC_T77	3648 × 2736	JPEG	100/200

$$x = \frac{x - min}{max - min} \tag{8}$$

For co-training and tri-transfer learning, we use the standard scaler initialization in the equation(9). Therefore, the initial accuracy of CCA and tri-transfer learning are different. We also found that CCA is invalid when it uses standard scaler initialization.

$$x = \frac{x - \mu}{\delta} \tag{9}$$

To evaluate the effect of TTL in mismatched JPEG compression, we compress the source and target images with standard quantization tables from 75 to 100 with an interval of 5. Therefore, we can obtain T_{100}, T_{95}, T_{90}, T_{85} T_{80} and T_{75} of the training data. Similarly, we also have T_{100}, T_{95}, T_{90}, T_{85} T_{80} and T_{75} of the test data. The uncompressed data of the training and testing sets are named S_{Ori} and T_{Ori}, respectively. In practical forensic applications, the images we have are normally the original images. We conduct Experiment 1 by setting the original images as the training data and the compressed images as the testing images. The classifiers are built on S_{Ori} and applied to compressed sets T_{Ori}, T_{100}, T_{95}, T_{90}, T_{85} T_{80} and T_{75}. The initial and final results of TTL are shown in Table 3. Our method is suitable for conditions where training data are re-compressed. In Experiment 2, we use S_{95} and S_{85} to build identification models and then apply those to sets T_{Ori}, T_{100}, T_{95}, T_{90}, T_{85} T_{80} and T_{75}. The results are listed in Table 4-5. The compared methods have the same TTL setting. For every classification model, we set $ste = 1$ such that we select

Table 3 – Identification accuracy (%) when training data are not re-compressed.

	CCA						Co-training				Tri-transfer Learning					
	initial			final			initial		final		initial			final		
Train → Test	EDF	LBP	CFA	EDF	LBP	CFA	EDF	LBP	EDF	LBP	EDF	LBP	CFA	EDF	LBP	CFA
$S_{Ori} \rightarrow T_{Ori}$	74.03	83.35	83.11	73.95	83.88	82.94	77.61	85.12	85.50	85.85	78.64	87.23	85.11	95.32	95.70	**95.88**
$S_{Ori} \rightarrow T_{100}$	58.91	72.82	54.38	62.85	79.32	53.79	65.38	80.94	75.50	76.05	64.67	80.94	52.79	92.47	**93.29**	92.88
$S_{Ori} \rightarrow T_{95}$	27.47	42.64	39.62	45.38	53.44	40.21	46.76	53.74	57.85	58.38	45.82	53.73	39.41	78.88	79.12	**79.18**
$S_{Ori} \rightarrow T_{90}$	25.09	35.88	24.62	24.50	34.44	23.70	25.94	35.88	30.00	29.68	25.09	35.88	24.62	48.82	49.32	**49.94**
$S_{Ori} \rightarrow T_{85}$	15.94	25.06	10.56	17.56	24.74	12.76	18.58	23.64	19.05	20.23	18.44	23.64	12.38	29.03	29.91	**30.20**
$S_{Ori} \rightarrow T_{80}$	11.00	15.29	7.47	14.59	16.71	10.56	16.58	16.20	15.44	16.02	15.70	16.20	9.44	21.82	21.35	**22.41**
$S_{Ori} \rightarrow T_{75}$	7.55	11.70	6.88	11.29	12.02	9.02	12.76	12.44	11.68	11.70	11.91	10.97	6.35	9.14	**9.35**	8.85
Ave	31.42	40.96	32.37	35.72	43.50	32.37	37.65	43.99	42.20	42.55	37.17	44.08	32.87	53.64	53.99	**54.18**

Table 4 – Identification accuracy (%) when training data are re-compressed with quality factor of 95.

	CCA						Co-training				Tri-transfer Learning					
	initial			final			initial		final		initial			final		
Train → Test	EDF	LBP	CFA	EDF	LBP	CFA	EDF	LBP	EDF	LBP	EDF	LBP	CFA	EDF	LBP	CFA
$S_{95} \rightarrow T_{Ori}$	46.74	54.65	45.62	51.29	61.82	45.18	55.06	63.00	71.11	71.70	55.65	63.03	46.44	90.97	**91.09**	90.32
$S_{95} \rightarrow T_{100}$	49.08	48.55	69.59	59.79	62.18	72.56	63.97	63.94	75.05	74.52	63.82	63.94	76.09	91.82	92.50	**92.79**
$S_{95} \rightarrow T_{95}$	62.67	78.35	73.79	63.26	77.73	73.88	68.53	80.73	77.07	78.61	69.91	80.74	80.21	90.59	91.38	**91.76**
$S_{95} \rightarrow T_{90}$	36.44	31.47	42.21	32.79	36.23	45.74	36.54	48.74	46.62	48.62	36.44	48.74	37.68	62.47	**63.00**	62.47
$S_{95} \rightarrow T_{85}$	23.79	22.91	19.71	22.41	25.97	24.85	24.47	25.70	26.38	26.64	24.35	25.70	27.55	35.50	35.29	**36.32**
$S_{95} \rightarrow T_{80}$	17.61	14.94	13.79	19.26	18.73	17.41	21.06	17.08	20.12	19.64	20.64	17.08	18.26	27.56	28.82	**28.94**
$S_{95} \rightarrow T_{75}$	12.91	11.26	9.58	14.26	13.52	11.35	15.23	12.79	16.47	16.88	13.76	12.79	11.82	18.14	**18.50**	18.17
Ave	35.59	37.44	39.17	37.57	42.31	41.56	40.68	44.56	42.54	48.08	40.64	44.57	42.57	59.57	60.08	**60.11**

one sample from each category and add the samples to the training data in other classifiers in each iteration. In addition, we take the accuracy of the 160-th iteration as the final result.

4.2. *Results and discussions*

To evaluate the effectiveness of our method, we conduct extensive experiments under different conditions. The initial and final classification accuracy of TTL and other baseline methods are listed in Table 3-5. The highest accuracy for each mismatched task is highlighted.

4.2.1. *Experiment 1:*

For Experiment 1, the training data are original images, and the testing data are all re-compressed with different quantization tables. The results are listed in Table 3. It is observed that TTL has the best performance compared with other methods under this condition. CCA and co-training are effective, but the effect is far inferior to tri-transfer learning. For S_{Ori} to T_{90} and T_{95}, the initial accuracies of classifiers are lower than 0.5, which violates the assumption of co-training. Compared with co-training, the proposed method gains a significant improvement. Even if the initial accuracy of TTL is approximately 30%, TTL can guarantee a beneficial effect on the algorithm. Fig. 4 shows the results of each iteration in the condition S_{Ori} to T_{90}. For S_{Ori} to $T_{95} - T_{Ori}$, although the accuracies of classifiers are higher, TTL with the proposed constraints to select samples is more accurate than co-training. The result of each iteration of TTL is shown in Fig. 5 Therefore, TTL also performs better than co-training.

For the condition $\eta < 0.5$, Fig. 6 shows the comparison of TTL and co-training for S_{Ori} to T_{90}. Similarly, Fig. 7 shows the comparison between TTL and co-training for S_{Ori} to T_{95} under the condition $\eta > 0.5$. Here, the reason why we used S_{Ori} to T_{90} and T_{95} as examples is that they represent low initial accuracy and high initial accuracy, respectively.

In Fig. 4, the selection accuracies for each view are low and sometimes they are even lower than 0.5. However, the identification accuracy of TTL can continue increasing because of the constraints. As the data distribution of the target domain and the source domain continues to increase, the identification accuracy and the selection accuracy increase. In addition, we determine whether it is EDF, LBP or CFA, the identification accuracies of h_A, h_B and h_C become closer and each eventually converges to a certain value.

Fig. 5 shows the condition of $\eta > 0.5$. Although the selection accuracy is high, the pseudolabel for the most confident samples may still have errors. The constraint can also help to select more accurate samples.

Fig. 6 and Fig. 7 show the comparison of tri-transfer learning and co-training for S_{Ori} to T_{90} and T_{95} with view LBP and EDF. For testing data of T_{90}, the identification accuracy of co-training drops and converges to a lower accuracy than the original accuracy. However, for Tri-transfer learning, the result shows a higher convergence trend. Moreover, the performance of TTL is obviously better than co-training.

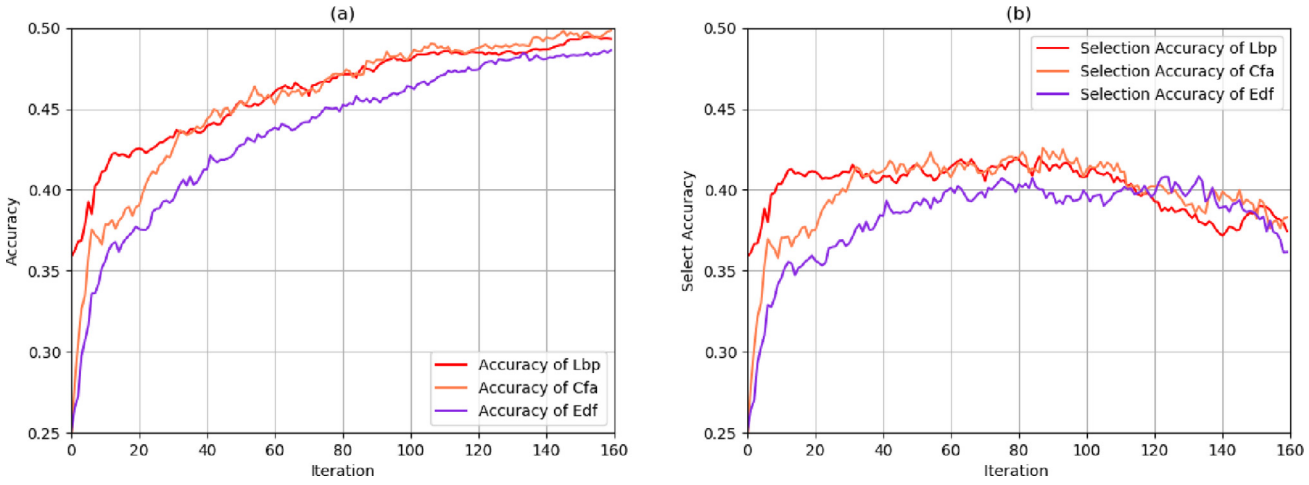

Fig. 4 – The accuracy of each iteration for S_{Ori} to T_{90}. (a) The accuracy of Classifier h_A for LBP.The accuracy of Classifier h_B for CFA.The accuracy of Classifier h_C for EDF. (b) The selection accuracy of h_A, h_B, h_C for the remaining samples after selection.

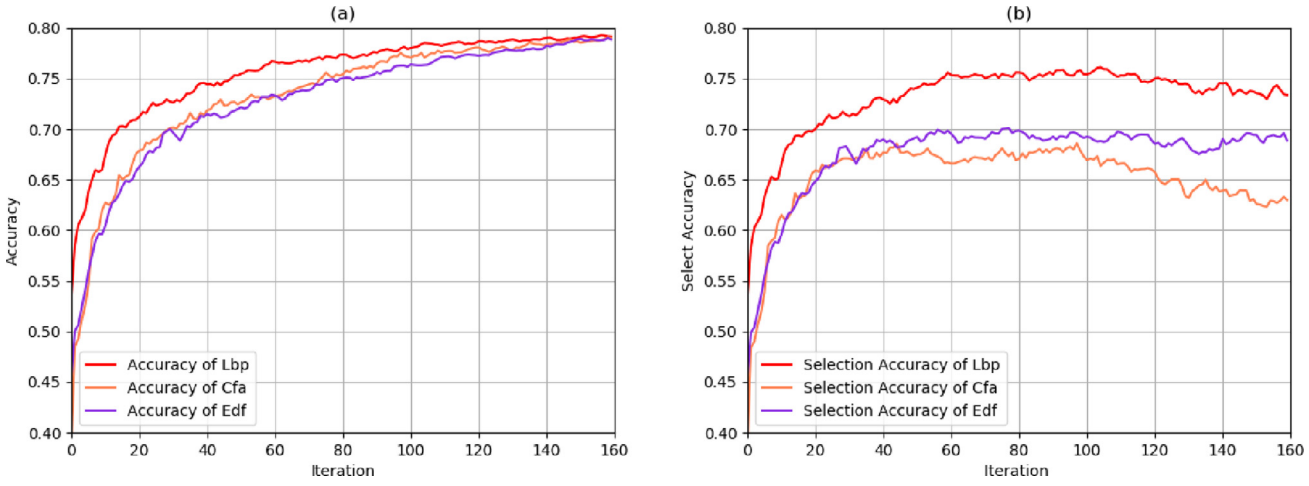

Fig. 5 – The accuracy of each iteration for S_{Ori} to T_{95}. (a) The accuracy of Classifier h_A for LBP.The accuracy of Classifier h_B for CFA.The accuracy of Classifier h_C for EDF. (b) The selection accuracy of h_A, h_B, h_C for the remaining samples after selection.

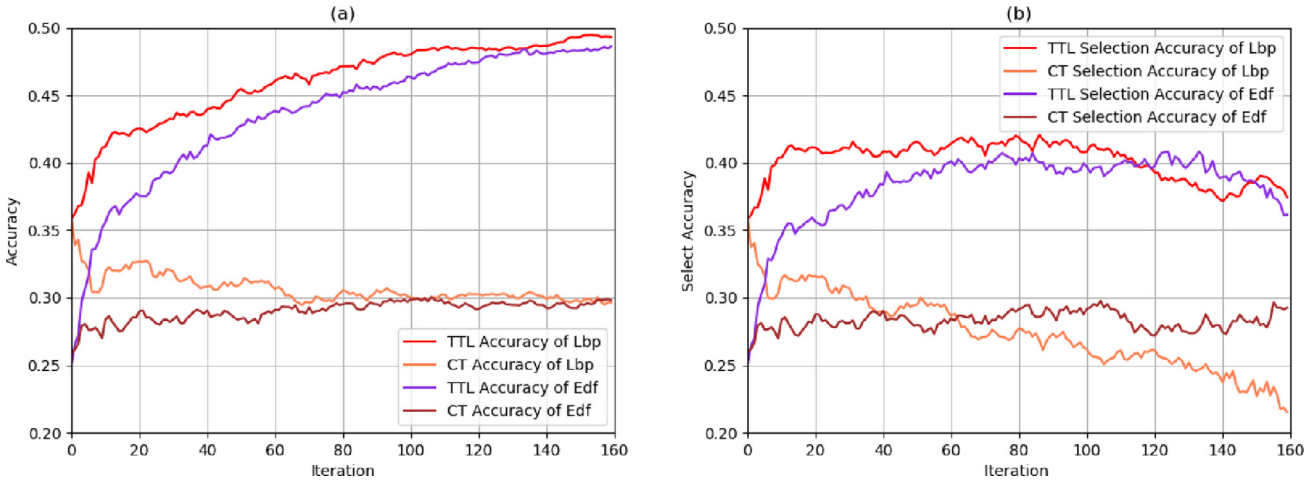

Fig. 6 – The accuracy of each iteration for S_{Ori} to T_{90}. (a) The accuracies of TTL and co-training for EDF. (b) The accuracies of TTL and Co-training for LBP.

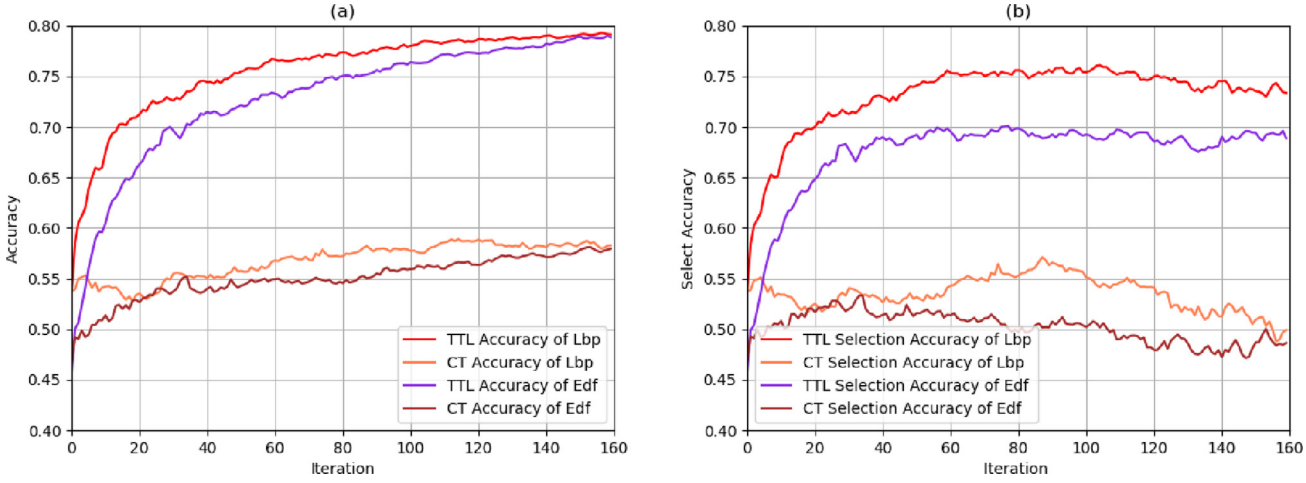

Fig. 7 – The accuracy of each iteration for S_{Ori} to T_{95}. (a) The accuracies of TTL and co-training for EDF. (b) The accuracies of TTL and Co-training for LBP.

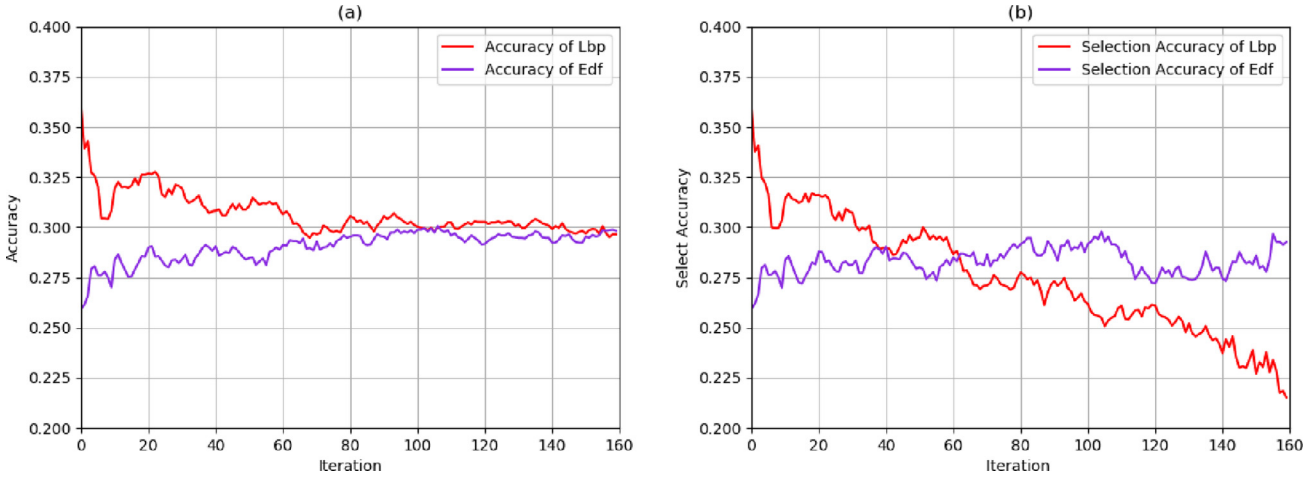

Fig. 8 – The accuracy of each iteration for S_{Ori} to T_{90}. (a) The accuracy of Classifier h_A of LBP.The accuracy of Classifier h_B for EDF.(b)The selection accuracy of h_A, h_B, h_C for the remaining samples after selection.

Fig. 8 and Fig. 9 show the classifier accuracy and selection accuracy of co-training for S_{Ori} to T_{90} and T_{95}. For the test data of 90, we see that if the value of selection accuracy is low to a certain degree, it will negatively impact on identification accuracy. However, when the selection accuracy is high enough, the co-training performance is not satisfactory in the case that the identification accuracy is also high. Comparing the selection accuracy of tri-transfer learning in Fig. 4 and that of co-training in Fig. 8, it is not difficult to explain why tri-transfer learning performs better.

We can also find that TTL fails with quality factors lower than 75% in Table 3. It shows that certain conditions are required for TTL to be effective.

4.2.2. *Experiment 2:*

For Experiment 2, the training samples are also re-compressed, and the experimental results are shown in Table 4-5.

We notice that the traditional forensic methods perform better when the training set and the testing set are matched. However, the larger the domain shift is, the poorer the result. Compared with co-training and CCA, the TTL performs best in all the condition. Simultaneously, we also find some interesting results.

First, the final results of TTL often depend on the distribution of the target data and the gap between the target domain and source domain. Taking the training data of S_{95} as an example, we notice that the initial accuracy is the highest when the test data are T_{95}, which means that the training data and test data are matched. However, the final results of S_{95} to T_{100} are better. The phenomena can also be found in other training data with different quantization tables in Table 5.

Second, when the gap between the training data and testing data is too large, the results are greatly affected. As shown in Table 8, the accuracies of S_{85} to T_{100}, T_{95}, T_{90} are only 76.54%, 78.13% and 80.38%, respectively. If the gap is in a certain range that the selection accuracy is sufficient to ensure that the se-

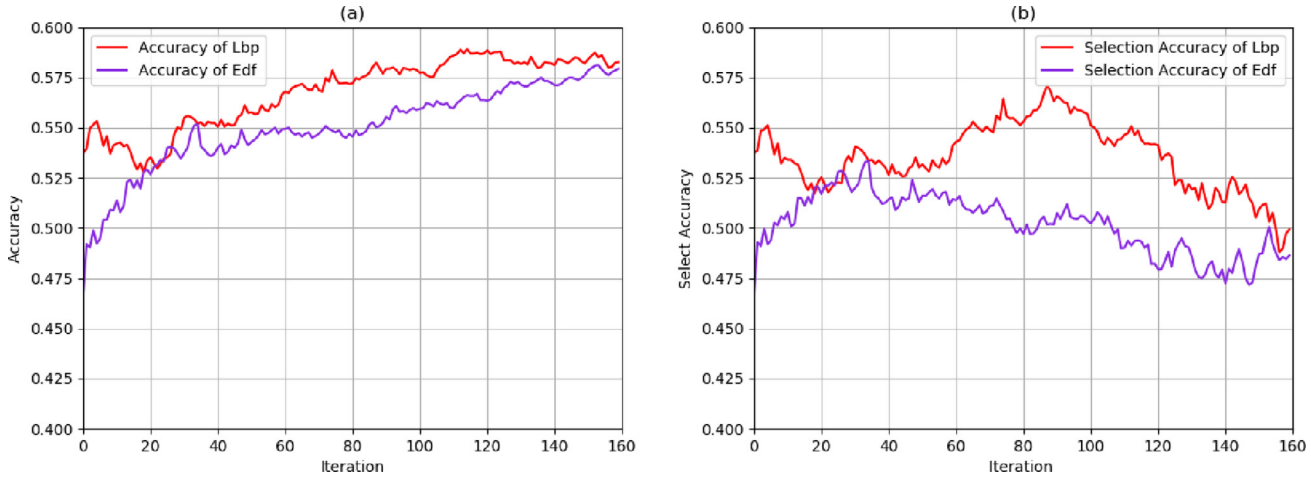

Fig. 9 – The accuracy of each iteration for S_{Ori} to T_{95}. (a) The accuracy of Classifier h_A of LBP.The accuracy of Classifier h_B for EDF (b)The selection accuracy of h_A, h_B, h_C for the remaining samples after selection.

Table 5 – Identification accuracy (%) when training data are re-compressed with quality factor of 85.

	CCA						Co-training				Tri-transfer Learning					
	initial			final			initial		final		initial			final		
Train → Test	EDF	LBP	CFA	EDF	LBP	CFA	EDF	LBP	EDF	LBP	EDF	LBP	CFA	EDF	LBP	CFA
$S_{85} \rightarrow T_{Ori}$	19.55	31.32	18.59	20.29	33.18	28.32	23.00	35.85	32.79	32.32	23.17	35.85	28.08	60.29	61.70	**63.47**
$S_{85} \rightarrow T_{100}$	21.73	24.76	24.59	23.76	33.79	39.59	27.06	37.70	34.58	34.17	28.82	37.70	44.38	69.85	70.79	**72.35**
$S_{85} \rightarrow T_{95}$	24.15	22.14	25.53	26.44	34.74	36.71	28.76	35.88	35.20	36.76	30.97	35.88	40.94	65.50	66.44	**67.00**
$S_{85} \rightarrow T_{90}$	32.88	38.41	32.00	35.85	42.88	34.17	39.97	49.03	46.26	48.44	42.61	49.03	41.32	71.73	72.67	**74.08**
$S_{85} \rightarrow T_{85}$	49.03	61.68	43.23	49.94	60.17	43.44	53.38	69.00	60.02	61.90	57.32	69.00	53.73	76.76	**78.26**	77.41
$S_{85} \rightarrow T_{80}$	29.00	38.09	28.68	31.18	41.32	29.53	35.14	45.47	38.88	40.53	37.32	45.50	35.88	52.79	**53.85**	51.64
$S_{85} \rightarrow T_{75}$	20.08	22.03	20.06	25.26	29.61	22.20	29.32	32.47	30.08	31.32	30.41	32.47	27.14	37.76	**38.88**	38.70
Ave	28.06	34.05	27.52	30.38	39.38	33.42	33.80	43.62	39.68	40.77	35.80	43.63	38.78	62.09	63.22	**63.51**

lected samples contribute to the classifiers, the result is exciting.

5. Conclusion

In this paper, we propose a novel iterative algorithm tri-transfer learning for the mismatched camera model identification of re-compressed images. TTL aims to fill the gap between the training data and testing data by labelling the test samples and adding them to the training data with pseudo-labels. Many experiments on the Dresden Image Database and synthetic data show the effectiveness of TTL compared with co-training and other algorithms. The results show that TTL outperforms several state-of-the-art methods on mismatched camera model identification.

Declaration of Competing Interest

The authors declare that they do not have any financial or nonfinancial conflict of interests.

CRediT authorship contribution statement

Guowen Zhang: Conceptualization, Methodology, Software. **Bo Wang:** Supervision, Project administration. **Fei Wei:** Data curation, Writing - original draft. **Kaize Shi:** Software, Validation. **Yue Wang:** Visualization, Investigation. **Xue Sui:** Writing - review & editing. **Meineng Zhu:** Writing - review & editing.

Acknowledgments

This work was supported by the National Natural Science Foundation of China (No. U1936117, No. U1736119 and No. 61772111).

Supplementary material

Supplementary material associated with this article can be found, in the online version, at doi:10.1016/j.cose.2020.102076.

REFERENCES

Angluin D, Laird P. Learning from noisy examples. Mach. Learn. 1988;2(4):343–70.

Balcan M-F, Blum A, Yang K. Co-training and expansion: Towards bridging theory and practice. In: Advances in neural information processing systems; 2005. p. 89–96.

Bayram S, Sencar H, Memon N, Avcibas I. Source camera identification based on cfa interpolation. IEEE International Conference on Image Processing, 2005. pp. III–69–72.

Bhatt HS, Bharadwaj S, Singh R, Vatsa M, Noore A, Ross A. On co-training online biometric classifiers. In: International Joint Conference on Biometrics; 2011. p. 1–7.

Bhatt HS, Singh R, Vatsa M, Ratha NK. Improving cross-resolution face matching using ensemble-based co-transfer learning. IEEE Trans. Image Process. 2014;23(12):5654–69.

Blitzer J, Dredze M, Pereira F. Biographies, bollywood, boomboxes and blenders: domain adaptation for sentiment classification. Acl 2007;31(2):187–205.

Blum A, Mitchell T. Combining labeled and unlabeled data with co-training. In: Proceedings of the eleventh annual conference on Computational learning theory. ACM; 1998. p. 92–100.

Chen C, Stamm MC. Camera model identification framework using an ensemble of demosaicing features. In: Information Forensics and Security (WIFS), 2015 IEEE International Workshop on. IEEE; 2015. p. 1–6.

Chen M, Weinberger KQ, Blitzer J. Co-training for domain adaptation. In: Advances in neural information processing systems; 2011. p. 2456–64.

Dasgupta S, Littman ML, McAllester DA. Pac generalization bounds for co-training. In: Advances in neural information processing systems; 2002. p. 375–82.

Gloe T, Borowka K, Winkler A. Feature-based camera model identification works in practice. In: Information Hiding, International Workshop, Ih 2009, Darmstadt, Germany, June 8–10, 2009, Revised Selected Papers; 2009. p. 262–76.

Gloe T, Bhme R. The dresden image database for benchmarking digital image forensics. Journal of Digital Forensic Practice 2010;3(2):1584–90.

Goldman S, Zhou Y. Enhancing supervised learning with unlabeled data. In: ICML; 2000. p. 327–34.

Ho JS, Au OC, Zhou J, Guo Y. Inter-channel demosaicking traces for digital image forensics. In: IEEE International Conference on Multimedia and Expo; 2010. p. 1475–80.

Hu Y, Yu B, Jian C. Source camera identification using large components of sensor pattern noise. In: Computer Science and its Applications, 2009. CSA'09. 2nd International Conference on. IEEE; 2009. p. 1–5.

Hwa R, Osborne M, Sarkar A, Steedman M, Uk SEA. Corrected co-training for statistical parsers. In: Icml-03 Workshop on the Continuum From Labeled To Unlabeled Data in Machine Learning and Data Mining; 2003. p. 95–102.

Kai SC, Lam EY, Wong KKY. Source camera identification using footprints from lens aberration. Proceedings of SPIE - The International Society for Optical Engineering 2006;6069. 60690J–60690J–8

Kai SC, Lam EY, Wong KKY. Source camera identification by jpeg compression statistics for image forensics. In: TENCON 2006. 2006 IEEE Region 10 Conference; 2007. p. 1–4.

Kang X, Li Y, Qu Z, Huang J. Enhancing source camera identification performance with a camera reference phase sensor pattern noise. IEEE Trans. Inf. Forensics Secur. 2012;7(2):393–402.

Kharrazi M, Sencar HT, Memon N. Blind source camera identification, 1. IEEE; 2004. p. 709–12.

Kharrazi M, Sencar HT, Memon N. Blind source camera identification. In: International Conference on Image Processing; 2009. p. 709–12. Vol. 1

Kodovsky J, Fridrich J, Holub V. Ensemble classifiers for steganalysis of digital media. IEEE Trans. Inf. Forensics Secur. 2012;7(2):432–44.

Lawgaly A, Khelifi F, Bouridane A. Image sharpening for efficient source camera identification based on sensor pattern noise estimation. In: Emerging Security Technologies (EST), 2013 Fourth International Conference on. IEEE; 2013. p. 113–16.

Li C-T. Source camera identification using enhanced sensor pattern noise. IEEE Trans. Inf. Forensics Secur. 2010;5(2):280–7.

Li R. Learning based forensic techniques for source camera identification. Computer Science 2016.

Long M, Wang J, Ding G, Sun J, Yu PS. Transfer feature learning with joint distribution adaptation. In: IEEE International Conference on Computer Vision; 2014. p. 2200–7.

Lukas J, Fridrich J, Goljan M. Determining digital image origin using sensor imperfections, 5685. International Society for Optics and Photonics; 2005. p. 249–61.

Lukas J, Fridrich J, Goljan M. Digital camera identification from sensor pattern noise. IEEE Trans. Inf. Forensics Secur. 2006;1(2):205–14.

Ng MK, Wu Q, Ye Y. Co-transfer learning via joint transition probability graph based method. In: International Workshop on Cross Domain Knowledge Discovery in Web and Social Network Mining; 2012. p. 1–9.

Nigam K, Ghani R. Analyzing the effectiveness and applicability of co-training. In: International Conference on Information and Knowledge Management; 2000. p. 86–93.

Ojansivu V, Heikkil J. Blur insensitive texture classification using local phase quantization. In: International Conference on Image and Signal Processing; 2008. p. 236–43.

Pan SJ, Tsang IW, Kwok JT, Yang Q. Domain adaptation via transfer component analysis. IEEE Trans. Neural Networks 2011;22(2):199–210.

Pan SJ, Yang Q. A survey on transfer learning. IEEE Trans Knowl Data Eng 2010;22(10):1345–59.

Piva A. An overview on image forensics. ISRN Signal Processing 2013;2013.

Roy A, Chakraborty RS, Sameer U, Naskar R. Camera source identification using discrete cosine transform residue features and ensemble classifier. In: IEEE Conference on Computer Vision and Pattern Recognition Workshops; 2017. p. 1848–54.

Stamm MC, Wu M, Liu KR. Information forensics: an overview of the first decade. IEEE Access 2013;1:167–200.

Sutcu Y, Bayram S, Sencar HT, Memon N. Improvements on sensor noise based source camera identification. In: Multimedia and Expo, 2007 IEEE International Conference on. IEEE; 2007. p. 24–7.

Wan X. Co-training for cross-lingual sentiment classification. In: Joint Conference of the Meeting of the ACL and the International Joint Conference on Natural Language Processing of the Afnlp: Volume; 2009. p. 235–43.

Wang B, Guo Y, Kong X, Meng F. Source camera identification forensics based on wavelet features. In: Fifth International Conference on Intelligent Information Hiding and Multimedia Signal Processing; 2009. p. 702–5.

Wu G, Kang X, Liu KR. A context adaptive predictor of sensor pattern noise for camera source identification. In: Image Processing (ICIP), 2012 19th IEEE International Conference on. IEEE; 2012. p. 237–40.

Xu B, Wang X, Zhou X, Xi J, Wang S. Source camera identification from image texture features. Neurocomputing 2016;207:131–40.

Xu G, Shi YQ. Camera model identification using local binary patterns. In: Multimedia and Expo (ICME), 2012 IEEE International Conference on. IEEE; 2012. p. 392–7.

Xu J, He H, Man H. Dcpe co-training for classification. Neurocomputing 2012;86:75–85.

Zhang G, Wang B, Li Y. Cross-Class and inter-class alignment based camera source identification for re-compression images; 2017.
Zhao P, Hoi SCH. Otl: a framework of online transfer learning. In: International Conference on International Conference on Machine Learning; 2010. p. 1231–8.
Zhou Y, Goldman S. Democratic co-learning. In: IEEE International Conference on TOOLS with Artificial Intelligence; 2004. p. 594–602.
Zhou Z-H, Li M. Tri-training: exploiting unlabeled data using three classifiers. IEEE Trans. Knowl. Data Eng. 2005;17(11):1529–41.

Guowen Zhang received his B.S. degree from the School of Information and Communication Engineering at Dalian Unversity of Technology, Dalian, China in 2019, and he is currently pursuing his M.S. degree in the School of Information and Communication Engineering at Dalian Unversity of Technology. His current research interests focus on the areas of multimedia processing and security and person re-identification.

Bo Wang* received his B.S. degree in Electronic and Information Engineering, and his M.S.degree and Ph.D. degree in Signal and Information Processing from Dalian University of Technology, Dalian, China, in 2003, 2005 and 2010, respectively. From 2010 to 2012, he was a post-doctoral research associate in Faculty of Management and Economics in Dalian University of Technology. He is currently an Associate Professor in School of Information and Communication Engineering at Dalian University of Technology. His current research interests focus on the areas of multimedia processing and security, such as digital image processing and forensics.

Fei Wei received his B.S. degree in electrical engineering from Harbin University of Science and Technology, Harbin, China in 2012 and his M.S. degree in electrical engineering from Harbin Engineering University, Harbin, China in 2015. He is currently pursuing his Ph.D. degree in electrical engineering at the State University of New York at Buffalo, Buffalo, NY, USA.

Kaize Shi is currently pursuing his B.S. degree in Electronic and Communication Engineering from Dalian University of Technology, Dalian, China. His current research interest is image processing.

Yue Wang received her B.S. degree in Communication Engineering from Shenyang University of Technology, China, in 2019. She is currently pursuing her M.S. degree in Electronic and Communication Engineering from Dalian University of Technology, Dalian, China. Her current research interests are image processing and digital image forensics.

Xue Sui received his bachelor of science degree from northeast normal university in 1989, changchun, China; He obtained his doctorate in education from Liaoning normal university in Dalian, China in 2004. From 2004 to 2006, he did postdoctoral research in basic medicine in Shantou university. He is currently a professor at the college of psychology, Liaoning normal university. The area of research is behavioral decision making and neural mechanisms.

Meineng Zhu received his B.S. degree in Telecommunication, M.S. degree in Pattern Recognition and Intelligent System from Huazhong University of Science and Technology, Wuhan, China, in 2004 and 2007 respectively. He is currently an Associate Research Fellow in Beijing Institute of Electronics Technology and Application. His current research interests focus on the areas of multimedia processing and security, such as digital image processing and forensics.